Biocatalysis and Agricultural Biotechnology 17 (2019) 696–701

Contents lists available at ScienceDirect

Biocatalysis and Agricultural Biotechnology

journal homepage: www.elsevier.com/locate/bab

"Turn-on" fluorescent sensor-based probing of toxic Hg(II) and Cu(II) with potential intracellular monitoring

Tahir Rasheed[a], Faran Nabeel[a], Muhammad Adeel[a], Muhammad Bilal[b,*], Hafiz M.N. Iqbal[c,**]

[a] School of Chemistry & Chemical Engineering, State Key Laboratory of Metal Matrix Composites, Shanghai Jiao Tong University, 800 Dongchuan Road, 200240, Shanghai, China
[b] School of Life Science and Food Engineering, Huaiyin Institute of Technology, Huaian, China
[c] Tecnologico de Monterrey, School of Engineering and Sciences, Campus Monterrey, Ave. Eugenio Garza Sada 2501, Monterrey, N.L., CP 64849, Mexico

ARTICLE INFO

Keywords:
Rhodamine
Colorimetric
Toxic elements
Cytotoxicity
Bio-imaging

ABSTRACT

In this study, the synthesis of a "turn-on" fluorescent sensor 2-(6-bromobenzo[d]thiazol-2-yl)-3′,6′-bis(diethylamino)spiro[isoindoline-1,9′-xanthen]-3-one (BTDX), based on rhodamine and 2-amino-6-bromobenzothiazol was carried out. The introduction of different metal cations reveals that the sensor demonstrates highly selective "switch-on" colorimetric response for Hg (II) and Cu(II) in CH_3CN: H_2O (8:2 v/v) system. A substantial heightening of UV-Vis response attributed to the ring opening of xanthene moiety. This ring opening ascribed because of complexation between the analytes (Hg^{2+}/Cu^{2+}) and BTDX. Furthermore, the UV-Vis titration study reveals that the lower detection limit for Hg^{2+} and Cu^{2+} was as low as 4.9 μM and 3.36 μM along with the binding constant of $4.37 \times 10^5\,mol^{-1}$ and $4.6 \times 10^5\,mol^{-1}$, respectively. As a proof of concept, and promising applications in the biological field to detect Hg^{2+}, the newly developed sensor has proved its cell permeability with low toxicity and can be used for the intracellular monitoring of these toxic agents in HeLa cells. Therefore, the sensor can be regarded as an accurate fluorescent bio-imaging moiety in live HeLa cells via confocal microscopy.

1. Introduction

Heavy metals have been widely used at an industrial scale, which played an essential role in the development of human life. Nevertheless, their excessive use and discharge of large amounts of metal-contaminated wastewater have created serious issues for humans and the environment (Vil'pan et al., 2005; Hong et al., 2011; Bilal et al., 2018; Hernandez-Vargas et al., 2018; Rasheed et al., 2018a, 2018b; 2018f). Among all other heavy metals, mercury and copper are considered as most important metals for various industrial and biological processes. The concentration of mercury ions even at lower strengths is considered highly toxic compared to other heavy metal ions. It can damage human organs such as heart diseases, stomach disorder, kidneys failure, nervous breakdown, renal failure, and nose bleeding if present in the human body more than $5\,\mu g\,L^{-1}$ (Hoyle and Handy, 2005). Another form of mercury is methylmercury which is highly neurotoxic and produced by bacterial microorganisms mainly caused by sulfate-reducing bacteria. Methylmercury causes serious health issues such as Minamata, myocardial infarction, immune, endocrine, and nervous system impairment (Kim et al., 2012; Bera et al., 2014; Bhalla et al., 2012), resulting in gesture and perceptive complexities. Mercury accumulates in the environment through various transmitting channels, for example, water, food, and air which is alarming for aquatic, wild and human life. Therefore, a great deal of attention has been given to the detection of toxic elements such as mercury in the environment and biological systems (Hernandez-Vargas et al., 2018; Rasheed et al., 2018c, 2019a).

Copper is an important heavy metal and is a most abundant element in the human body after zinc (Zn^{2+}) and iron (Fe^{2+}) involved in the important interactions (Gaggelli et al., 2006; Turski and Thiele, 2009). Excess of copper, on the other hand, can cause serious troubles to normal body conditions (Domaille et al., 2008). Copper, if exposed to the human body for short duration can produce stomach problems, whereas its long-term exposure might harm kidney and liver (Barceloux and Barceloux, 1999; Valentine et al., 2005; Rasheed et al., 2018b). Accumulation of copper ions in the human body can cause Wilson's disease, amyloidal precipitation, prion and Parkinson's diseases (Wang et al., 2012; Kumari et al., 2014). Whereas, deficiency of copper ions in the body can enhance risks for heart diseases (Wang et al., 2014). Heavy metal ion detection in analytical chemistry and microorganisms

* Corresponding author.
** Corresponding author.
E-mail addresses: bilaluaf@hotmail.com (M. Bilal), hafiz.iqbal@tec.mx (H.M.N. Iqbal).

https://doi.org/10.1016/j.bcab.2019.01.032
Received 22 November 2018; Received in revised form 18 December 2018; Accepted 18 January 2019
Available online 25 January 2019
1878-8181/

is of foremost concern. Therefore, probing and measurement of mercury and copper ions have become indispensable to investigate their hazardous effects both on humans and the environment. In this context, several attempts have recently been made to design chemosensors for the detection of copper and mercury ions (Rasheed et al., 2019b; Lee et al., 2008; Chereddy and Thennarasu, 2011; Peng et al., 2011; Wang et al., 2011). Some mercury chemosensors are based on the thiophilicity (Zhu et al., 2008), although mercury detection in the sulfur-bearing environment increases the interaction of mercapto-chemicals.

Fluorescent visual detection by naked eye has frequently been used for the last decade because of simple operative, non-destructive, less expensive, and highly sensitive and selective nature (Vendrell et al., 2012; Erdemir and Kocyigit, 2015; Rasheed et al., 2018c, 2019a). Owing to higher molar extinction-coefficient, excellent spirolactam structural framework, extended absorption and emission wavelengths in the range of visible region and better fluorescence quantum yield (Φ) rhodamine-based chemosensors are considered as an ideal candidate for analyte detection (Chen et al., 2011; Zhu et al., 2015; Rasheed et al., 2017; Rasheed et al., 2018d). Rhodamine based chemosensors for detection of heavy metals have been synthesized of two kinds, i.e., spirocyclic ring (colorless) and open cycle (fluorescent) (Zhang et al., 2013; Dhara et al., 2014; Rasheed et al., 2018e), while most of them display enhanced fluorescence and useful for metal ion recognition (Zhang and Zhu, 2014; Yuan et al., 2015). However, few chemosensors are described in the literature which can detect two or more metal ions simultaneously (Zhao et al., 2011; Karakuş et al., 2014). Failure to recognize more metal ions at the same time perhaps present a drawback for these types of chemosensors. Keeping in mind the idea of detecting more than one metal ions, we developed a new rhodamine-based chemosensor BTDX in this study as illustrated in Scheme 1. BTDX is a rhodamine-based dual-analyte chemosensor, which can detect both mercury and copper metal ions as spirolactam compound by absorption (UV-visible) spectrum. Bi-cations recognition becomes essential when different signaling bands are involved as few templates can detect bi-cations.

2. Materials and methods

2.1. Reagents

The 2-amino-6-bromobenzothiazol and rhodamine B were obtained from Adamas chemical Co. Ltd. All analytical grade solvents were used as received during the experiments. All metal ions salts used in the spectroscopic measurements were mainly procured from Shanghai reagent company, China and Aldrich, USA. De-ionized water was used for all the experiments. Thin layer chromatography (TLC) was used for reaction monitoring.

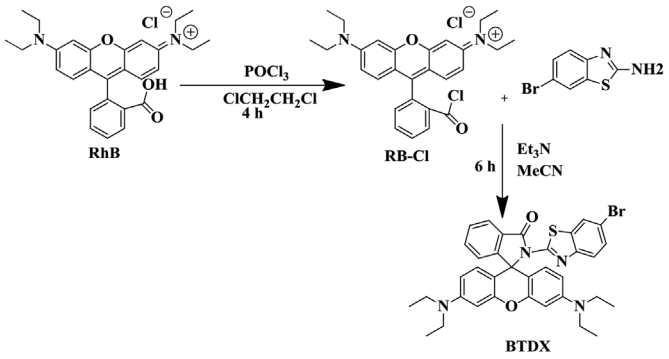

Scheme 1. Synthetic pathway of BTDX.

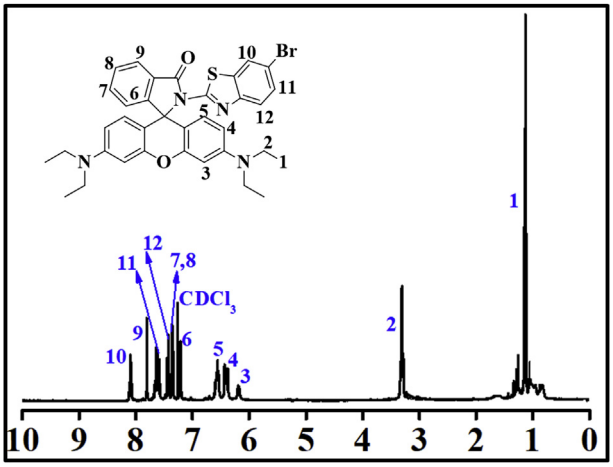

Fig. 1. ^{1}H NMR of BTDX in $CDCl_3$.

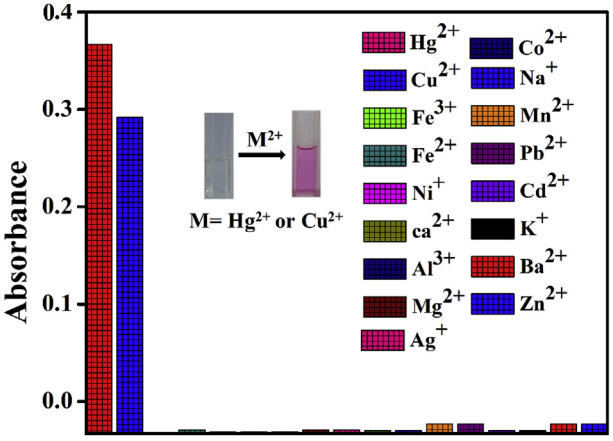

Fig. 2. UV-Visible response of BTDX (10 μM) towards Hg^{2+} and Cu^{2+} among miscellaneous metal cations in MeCN/H_2O (8:2 v/v).

2.2. Instrumentation

All the absorbance measurements were performed by using a Shimadzu UV-visible, spectrophotometer (UV- 2600). Mercury plus (400) spectrometer was used for NMR spectroscopy.

2.3. Spectroscopic measurements

All the stock solutions of metal ions with a concentration of 100 mM were prepared in deionized water from their nitrates, perchlorates, and chlorides. The BTDX stock solution was prepared with the concentration of 10 mM in acetonitrile/water co-solvent in 8:2 v/v. All the spectroscopic measurements (UV-visible) were performed at room temperature, and stock solution was also prepared and equilibrated at room temperature before spectroscopic analysis.

2.4. Cell culturing and bio-imaging

The HeLa cells were attained from School of Pharmacy of Shanghai Jiao Tong University, China and were cultured in DMEM (Dulbecco's Modified Eagle Medium) in the presence of 10% FBS (fetal bovine serum), Gibco and 1% antibiotic solution (Gibco) in an incubator (5% CO_2) at 37 °C. Before imaging, the cells were seeded for one day in flat bottom plates (96-well). After designated incubation time the 10 μM of BTDX was used to treat the cells for 1 h. Before imaging investigation, the known concentration (10 μM) of $Hg(NO_3)_2$ in ethanol and PBS (PBS: phosphate-buffered saline, 1:4, v/v) was added to each well for 30 min.

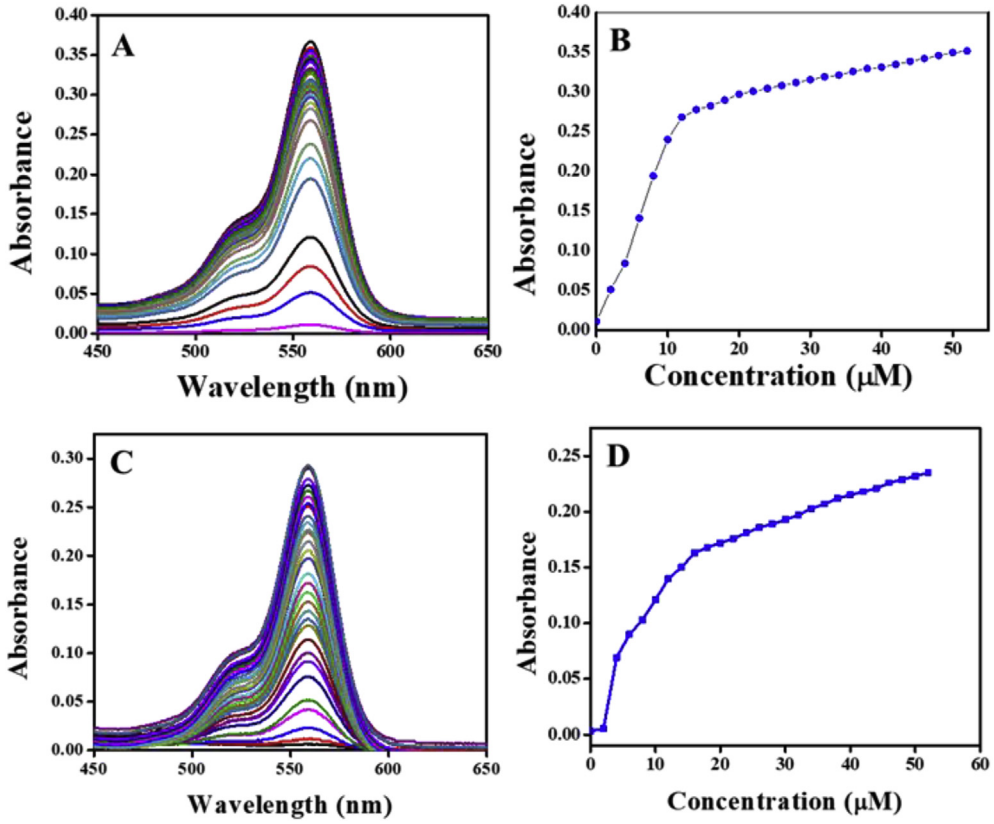

Fig. 3. (A, C) absorption titration spectra of BTDX (10 μM) in response to Hg^{2+} and Cu^{2+} (0.0–52 μM). (B, D) absorbance intensity variation at 559 nm on the altered concentration of Hg^{2+} and Cu^{2+}. The experiments were carried out in MeCN/H_2O (8:2 v/v).

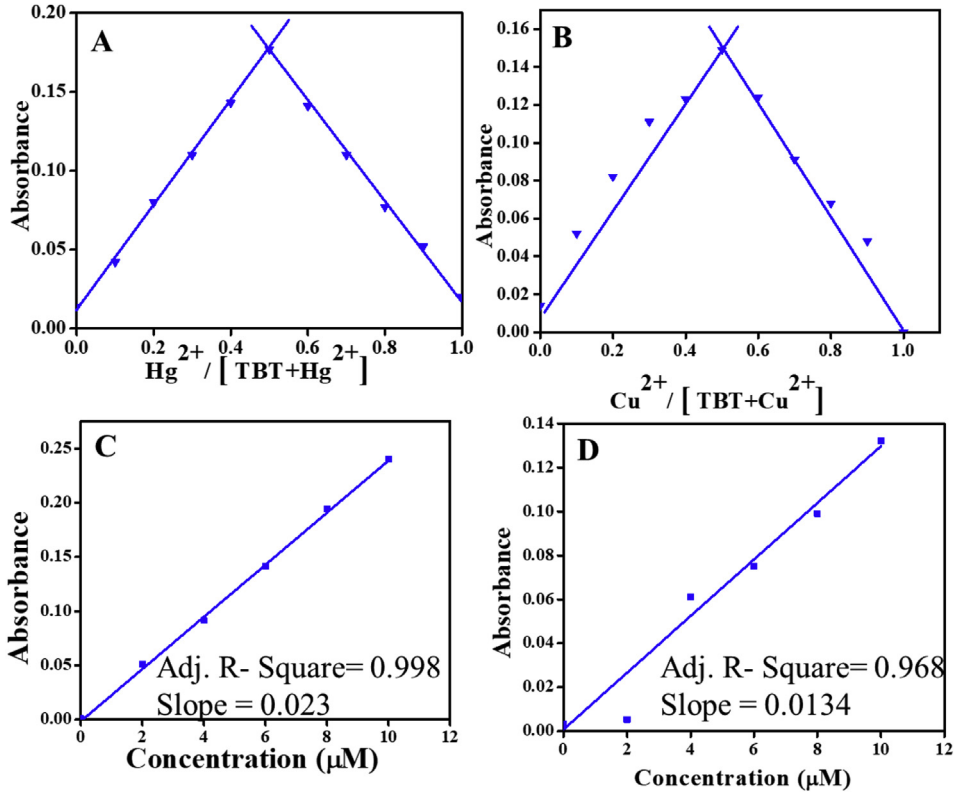

Fig. 4. (A, B) Job's plot to show 1:1 binding stoichiometry between Hg^{2+}/Cu^{2+} and BTDX. The total concentration of BTDX and metal ions remain 10 μM during the experiment. (C, D) linear relationship of the absorbance with the concentration of ions 0–10.0 μM. The absorbance values were taken at 559 nm.

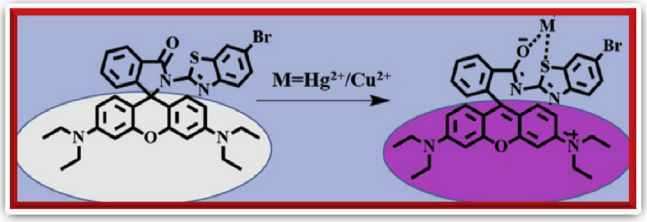

Scheme 2. Proposed binding mode of BTDX and analytes.

Finally, confocal laser microscope DMI-600, Germany, was used to take images of the treated cells using excitation wavelength equal to 550 nm under the dark and bright field.

3. Results and discussion

3.1. Synthesis of BTDX

The rhodamine B acid chloride was synthesized by a slight modification in the already reported procedure (Yang et al., 2011). Briefly, 1.0 g of rhodamine B (2.1 mM) was dissolved in 20 mL of dichloromethane (DCM) followed by dropwise addition of 4 mL of phosphorous oxychloride to the stirred solution of rhodamine B at room temperature, and the mixture was refluxed for 6 h with continuous stirring. After completion of the reaction, the mixture was cooled down to room temperature, and the solvent was removed under reduced pressure. The rhodamine B acid chloride obtained as a purple sticky solid was used without purification and characterization in the next step. The rhodamine B acid chloride obtained from the first step was dissolved in 10 mL of the anhydrous CH_3CN and stirred at room temperature, 10 mL of an anhydrous solution of Triethylamine (5 mL) and 2-amino-6-bromobenzothiazol 0.7 g (4.2 mM) was added dropwise for 30 min in an ice bath and then reflux the solution for 12 h. After that, the solution was cooled down to room temperature, and the mixture was poured into 50 mL of distilled water followed by extraction with DCM (6 × 20 mL) and dried over anhydrous Na_2SO_4. The organic layer was evaporated under reduced pressure, and the crude product was purified by column chromatography using DCM/CH3OH (9: 1 v/v) as an eluent. Compared to all other rhodamine-based chemical sensors; BTDX has been prepared efficiently and economically with 80% of yield. The schematic preparation of chemosensor BTDX is shown in Scheme 1. ^{1}H NMR spectrometry (Fig. 1) confirmed the formation of BTDX.

3.2. Spectral investigations

The absorption investigations were carried out using acetonitrile and water co-solvent (8:2 v/v) as a medium. The outcome of these investigations reveals that the as-prepared chemical sensor (BTDX 10 μM) is selective for Hg^{2+} and Cu^{2+} among different competitive cations. A turn-off response was observed when these competitive cations (100 μM) were introduced to the solution of 10 μM BTDX. While the addition of Hg^{2+} or Cu^{2+} causes a switch-on response to pink color prior to colorless. The change in color is clear and can be seen by open eye (Fig. 2).

A detailed spectroscopical study (UV–vis), was executed to further investigate the sensing behavior of BTDX. All the absorption spectra were performed in acetonitrile: H_2O (8:2 v/v) system. As expected, the blank BTDX solution shows no peaks for absorbance revealing the existence of BTDX (as rhodamine moiety) in spirocyclic form. On the contrary, a considerable amount of absorbance was witnessed at 559 nm upon addition of Hg^{2+} or Cu^{2+} (100 μM) solution to BTDX (10 μM) solution (Fig. 2). This enhanced absorption maximum indicates the presence of spirocyclic ring-opened configuration of the rhodamine moiety. This configuration is responsible for the change in color, i.e., colorless to a pink color, consolidating the fact that the BTDX can be regarded as "bare-eye" sensor for Hg^{2+} or Cu^{2+}. To have a better insight into the selectivity of BTDX, the spectral titration experiments were carried out. An enhanced absorbance response at 559 nm was observed by the continuing addition of 0–52 μM solution of Hg^{2+} or Cu^{2+} to BTDX solution (10 μM). This increase of absorbance response becomes saturated when 1.0 equivalent of metal ions were added (Fig. 3A and C).

3.3. Binding stoichiometry and complexation constant

The stoichiometries of complexation (BTDX-Hg^{2+} or BTDX-Cu^{2+}) were investigated by means of the method of constant variance (Job's plot method). As shown in Fig. 4A and B, the complexation ratio between analyte and probe is 1:1. The total concentration of the analyte and probe remains 10 μM during these calculations. Based on the binding stoichiometry, the binding constant values and lower limit of detections (LOD) were determined by using Equations (1) and (2). The absorption intensity data obtained as a result of UV-Visible absorption spectroscopy was used for these calculations (Fig. 3B and D).

$$A = (A_0 + A_{lim}K_nC_M^n) / (1 + K_nC_M^n) \quad (1)$$

$$LOD = 3\sigma/slope \quad (2)$$

Here, A_0, A_{lim} and A, are the intensity of absorption for blank BTDX, BTDX saturated with excess amount of Hg^{2+} and Cu^{2+}, and BTDX/metal ion complexes [BTDX + Hg^{2+}] or [BTDX + Cu^{2+}], respectively. C_M is the concentration of metal ions, and n is the stoichiometric ratio between metal ion and RBP complex formation. K_n is the binding constant. The value of binding constant determined for complexes BTDX-Hg^{2+} and BTDX-Cu^{2+} were $4.37 \times 10^6\ mol^{-1}$ and

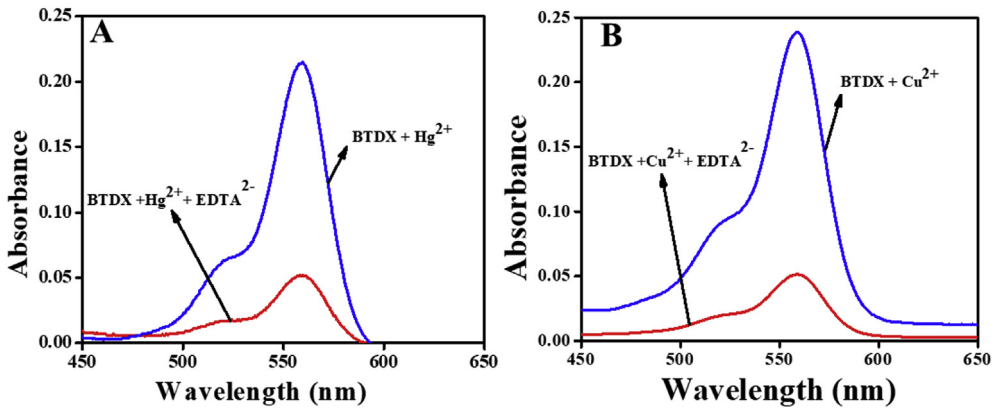

Fig. 5. The absorption spectra of BTDX-Hg^{2+} (A) and BTDX-Cu^{2+} (B) solutions (10.0 equiv. of metal ions) before and after the addition of 10.0 equiv. of $EDTA^{2-}$.

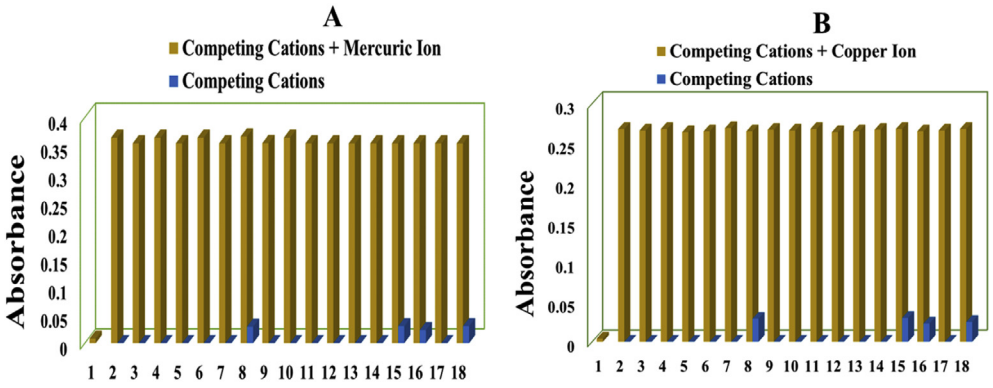

Fig. 6. Absorption intensities of BTDX (10 μM) at 559 nm, in presence of 10.0 equiv. of several cations (blue bars) and after further addition of 10.0 equiv. of Hg^{2+} (A) and Cu^{2+} (B) (brown bars). 1, Blank; 2, Ag^{+}; 3, Al^{3+}; 4, Ba^{2+}; 5, Ca^{2+}; 6, Cd^{2+}; 7, Fe^{3+}; 8, Fe^{2+}; 9, K^{+}; 10, Li^{+}; 11, Mg^{2+}; 12, Mn^{2+}; 13, Co^{2+}; 14, Pb^{2+}; 15, Ni^{2+}; 16, Na^{+}; 17, Zn^{2+}; 18, mixture of all metal ions.

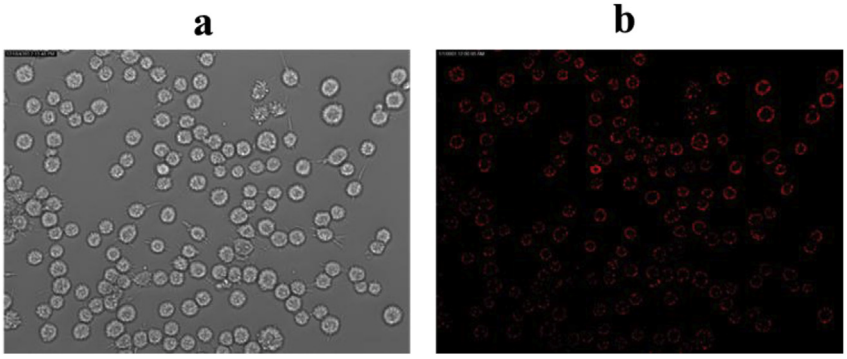

Fig. 7. Confocal laser pictographs of HeLa cells stained by 10 μM of (a) BTDX and (b) BTDX + Hg^{2+}.

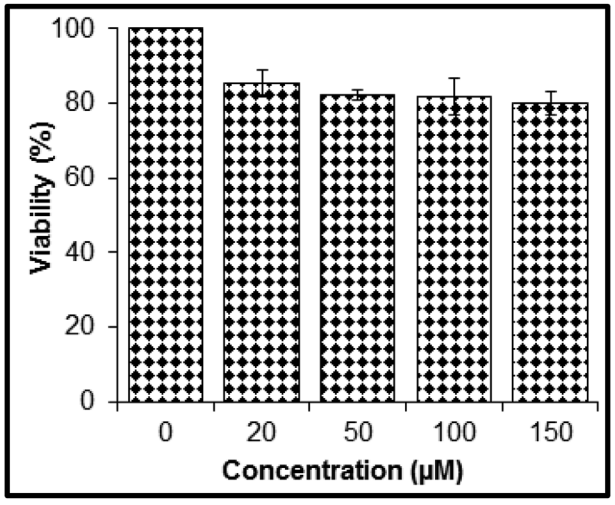

Fig. 8. Percentage viability of the HeLa cells.

$4.6 \times 10^5\ mol^{-1}$, respectively. Further, the LOD was calculated with the help of Equation (2) using a linear correlation (0–10 μM) between the concentration of the analyte and BTDX (Fig. 4C and D). The LOD values for Hg^{2+} and Cu^{2+} were determined as low as 4.9 μM and 3.36 μM, respectively.

3.4. Proposed binding mechanism

The proposed binding mechanism of the complies BTDX/Hg^{2+}, or Cu^{2+} is shown in Scheme 2. It was assumed that the oxygen atom of carbonyl group present on xanthene moiety and the sulfur atom of thiazole moiety might coordinate with the analyte (Hg^{2+} or Cu^{2+}) to establish spirocyclic ring opening of the rhodamine moiety (Yang et al., 2011).

3.5. Reversibility nature of BTDX/analyte complexation

The complex free ability of BTDX was proved by the addition of 100 mM of ethylenediaminetetraacetate (EDTA) solution to BTDX-Hg^{2+} or Cu^{2+} solution. In complexed form, the solution was pink in color, but when the EDTA solution was introduced to that solution, the color disappears. This disappearance of color indicates that the complexation between analyte and BTDX is reversible (Fig. 5a and b).

3.6. Interference study

The possible interference of miscellaneous cations such as Na^{+}, K^{+}, Ca^{2+}, Mg^{2+}, Cr^{3+}, Fe^{3+}, Al^{3+}, Mn^{2+}, Zn^{2+}, Pb^{2+}, Fe^{2+}, Co^{2+}, Ni^{2+}, Cd^{2+}, and Ag^{+} was investigated to prove the highly selective nature of BTDX. The outcomes of these investigations reveal that all the interfering cations do not affect the absorption maxima induced by Hg^{2+} or Cu^{2+}. Hence, we can conclude that the sensor could be useful as a selective probe for detection of Cu^{2+} and Hg^{2+} (Fig. 6A and 6B).

3.7. Cell imaging study

The live cell experiments were carried out using confocal laser microscope (DMI-6000, Leica, Germany). These investigations were performed using HeLa cell line. The BTDX cell permeability was measured by incubating the HeLa cell with BTDX (10 μM) for 1 h in the growth medium at 37 °C. Upon loading 1.0 equiv. of the analytes for 30 min, a clear fluorescence image was witnessed from an intracellular portion of HeLa cells (Fig. 7). Therefore, BTDX can be useful for intracellular investigation of Hg^{2+} in-vitro bioactivity in living organisms for toxicity analysis of Hg^{2+}.

3.8. Cytotoxicity assay

The conventional MTT assay was performed for the % age viability of the cells. The HeLa cells were trypsinized in 96-well culture plates.

The final concentration of the cell was 3.0×10^3 cells per well in 200 µL DMEM (Dulbecco's Modified Eagle's Medium) complete medium. The cells were permitted to stick to the bottom upon their growth at 37 °C for 24 h in a CO_2 incubator (Thermo Fisher Scientific). Finally, variable concentrations of a sensor (0–150 µM) were supplemented to the wells and retained in an incubator for 24 h. Additionally, 10 µL of 1.0 mg/mL sterile filtered 3-(4, 5 -dimethylthiazol-2-yl)-2, 5-diphenyl tetrazolium bromide (MTT) reagent in phosphate-buffered saline (PBS, pH 7.4) were added to each well and allowed to incubate for 6.0 h. The active mitochondria of live cells reduce MTT to purple formazan. The insoluble formazan precipitates were dissolved in 200 µL/well dimethylsulfoxide (DMSO) which was then measured Spectrophotometrically in a microplate reader (2300 EnSpire Multilabel Plate Reader-Perkin Elmer, USA) at 580 nm. The cytotoxic effect of each treatment was expressed as a percentage of cell viability about the untreated control cells. All the experiments were performed in quadruplet for each concentration. It can be seen in Fig. 8 that the percentage viability was not less than 80%.

4. Conclusions

The present research reported a new kind of rhodamine-based chemosensor BTDX for the detection of Hg^{2+} and Cu^{2+} in living systems and an aqueous medium. The experimental findings propose BTDX an excellent selective colorimetric sensor which detects Hg^{2+} and Cu^{2+}. BTDX is a kind of single molecular sensor and can recognize bication with different spectral bands. The results of the spectral and fluorescence findings show that BTDX can be used for detection and monitoring of Hg^{2+} in living systems. Hence, BTDX can work well as chemosensor in the medical filed.

Conflicts of interest

All authors are happy to declare that there is no conflict of interest in any capacity either competing or financial.

Acknowledgments

The authors are grateful to the School of Chemistry & Chemical Engineering, State Key Laboratory of Metal Matrix Composites, and School of Life Science and Food Engineering, Huaiyin Institute of Technology, Huaian, China for providing experimental facilities.

References

Barceloux, D.G., Barceloux, D., 1999. Copper. J. Toxicol. Clin. Toxicol. 37 (2), 217–230.
Bera, K., Das, A.K., Nag, M., Basak, S., 2014. Development of a rhodamine–rhodanine-based fluorescent mercury sensor and its use to monitor real-time uptake and distribution of inorganic mercury in live zebrafish larvae. Anal. Chem. 86 (5), 2740–2746.
Bhalla, V., Roopa, Kumar, M., Sharma, P.R., Kaur, T., 2012. New fluorogenic sensors for Hg2+ ions: through-bond energy transfer from pentaquinone to rhodamine. Inorg. Chem. 51, 2150–2156.
Bilal, M., Rasheed, T., Sosa-Hernández, J., Raza, A., Nabeel, F., Iqbal, H., 2018. Biosorption: an interplay between marine algae and potentially toxic elements—a review. Mar. Drugs 16 (2), 65.
Chen, X., Pradhan, T., Wang, F., Kim, J.S., Yoon, J., 2011. Fluorescent chemosensors based on spiroring-opening of xanthenes and related derivatives. Chem. Rev. 112 (3), 1910–1956.
Chereddy, N.R., Thennarasu, S., 2011. Synthesis of a highly selective bis-rhodamine chemosensor for naked-eye detection of Cu2+ ions and its application in bio-imaging. Dyes Pigments 91 (3), 378–382.
Dhara, A., Jana, A., Guchhait, N., Ghosh, P., Kar, S.K., 2014. Rhodamine-based molecular clips for highly selective recognition of Al 3+ ions: synthesis, crystal structure and spectroscopic properties. New J. Chem. 38 (4), 1627–1634.
Domaille, D.W., Que, E.L., Chang, C.J., 2008. Synthetic fluorescent sensors for studying the cell biology of metals. Nat. Chem. Biol. 4 (3), 168.
Erdemir, S., Kocyigit, O., 2015. Reversible "OFF–ON" fluorescent and colorimetric sensor based benzothiazole-bisphenol A for fluoride in MeCN. Sensor. Actuator. B Chem. 221, 900–905.
Gaggelli, E., Kozlowski, H., Valensin, D., Valensin, G., 2006. Copper homeostasis and neurodegenerative disorders (Alzheimer's, prion, and Parkinson's diseases and amyotrophic lateral sclerosis). Chem. Rev. 106 (6), 1995–2044.
Hernandez-Vargas, G., Sosa-Hernández, J., Saldarriaga-Hernandez, S., Villalba-Rodríguez, A., Parra-Saldivar, R., Iqbal, H., 2018. Electrochemical biosensors: a solution to pollution detection with reference to environmental contaminants. Biosensors 8 (2), 29.
Hong, K.S., Lee, H.M., Bae, J.S., Ha, M.G., Jin, J.S., Hong, T.E., et al., 2011. Removal of heavy metal ions by using calcium carbonate extracted from starfish treated by protease and amylase. J Anal Sci Technol 2 (2), 75–82.
Hoyle, I., Handy, R.D., 2005. Dose-dependent inorganic mercury absorption by isolated perfused intestine of rainbow trout, Oncorhynchus mykiss, involves both amiloride-sensitive and energy-dependent pathways. Aquat. Toxicol. 72 (1–2), 147–159.
Karakuş, E., Üçüncü, M., Emrullahoğlu, M., 2014. A rhodamine/BODIPY-based fluorescent probe for the differential detection of Hg (II) and Au (III). Chem. Commun. 50 (9), 1119–1121.
Kim, H.N., Ren, W.X., Kim, J.S., Yoon, J., 2012. Fluorescent and colorimetric sensors for detection of lead, cadmium, and mercury ions. Chem. Soc. Rev. 41 (8), 3210–3244.
Kumari, N., Dey, N., Bhattacharya, S., 2014. Remarkable role of positional isomers in the design of sensors for the ratiometric detection of copper and mercury ions in water. RSC Adv. 4 (9), 4230–4238.
Lee, M.H., Kim, H.J., Yoon, S., Park, N., Kim, J.S., 2008. Metal ion induced FRET OFF−ON in Tren/Dansyl-appended rhodamine. Org. Lett. 10 (2), 213–216.
Peng, X., Wang, Y., Tang, X., Liu, W., 2011. Functionalized magnetic core–shell Fe3O4@SiO2 nanoparticles as selectivity-enhanced chemosensor for Hg (II). Dyes Pigments 91 (1), 26–32.
Rasheed, T., Bilal, M., Iqbal, H.M., Hu, H., Zhang, X., 2017. Reaction mechanism and degradation pathway of rhodamine 6G by photocatalytic treatment. Water, Air, Soil Pollut. 228 (8), 291.
Rasheed, T., Bilal, M., Nabeel, F., Iqbal, H.M., Li, C., Zhou, Y., 2018a. Fluorescent sensor based models for the detection of environmentally-related toxic heavy metals. Sci. Total Environ. 615, 476–485.
Rasheed, T., Li, C., Bilal, M., Yu, C., Iqbal, H.M., 2018b. Potentially toxic elements and environmentally-related pollutants recognition using colorimetric and ratiometric fluorescent probes. Sci. Total Environ. 640, 174–193.
Rasheed, T., Li, C., Zhang, Y., Nabeel, F., Peng, J., Qi, J., et al., 2018c. Rhodamine-based multianalyte colorimetric probe with potentialities as on-site assay kit and in biological systems. Sensor. Actuator. B Chem. 258, 115–124.
Rasheed, T., Bilal, M., Iqbal, H.M., Shah, S.Z.H., Hu, H., Zhang, X., Zhou, Y., 2018d. TiO2/UV-assisted rhodamine B degradation: putative pathway and identification of intermediates by UPLC/MS. Environ. Technol. 39 (12), 1533–1543.
Rasheed, T., Li, C., Nabeel, F., Qi, M., Zhang, Y., Yu, C., 2018e. Real-time probing of mercury using an efficient "turn-on" strategy with potential as in-field mapping kit and in live cell imaging. New J. Chem. 42, 10940–10946.
Rasheed, T., Li, C., Fu, L., Nabeel, F., Yu, C., Gong, L., Zhou, Y., 2018f. Development and characterization of newly engineered chemosensor with intracellular monitoring potentialities and lowest detection of toxic elements. J. Mol. Liq. 272, 440–449.
Rasheed, T., Li, C., Nabeel, F., Huang, W., Zhou, Y., 2019a. Self-assembly of alternating copolymer vesicles for the highly selective, sensitive and visual detection and quantification of aqueous Hg2+. Chem. Eng. J. 358, 101–109.
Rasheed, T., Nabeel, F., Li, C., Zhang, Y., 2019b. Rhodol assisted alternating copolymer based chromogenic vesicles for the aqueous detection and quantification of hydrazine via switch-on strategy. J. Mol. Liq. 274, 461–469.
Turski, M.L., Thiele, D.J., 2009. New roles for copper metabolism in cell proliferation, signaling, and disease. J. Biol. Chem. 284 (2), 717–721.
Valentine, J.S., Doucette, P.A., Zittin Potter, S., 2005. Copper-zinc superoxide dismutase and amyotrophic lateral sclerosis. Annu. Rev. Biochem. 74, 563–593.
Vendrell, M., Zhai, D., Er, J.C., Chang, Y.T., 2012. Combinatorial strategies in fluorescent probe development. Chem. Rev. 112 (8), 4391–4420.
Vil'pan, Y.A., Grinshtein, I.L., Akatov, A.A., Gucer, S., 2005. Direct atomic absorption determination of mercury in drinking water and urine using a two-step electrothermal atomizer. J. Anal. Chem. 60 (1), 38–44.
Wang, H.H., Xue, L., Yu, C.L., Qian, Y.Y., Jiang, H., 2011. Rhodamine-based fluorescent sensor for mercury in buffer solution and living cells. Dyes Pigments 91 (3), 350–355.
Wang, J., Li, H., Long, L., Xiao, G., Xie, D., 2012. Fast responsive fluorescence turn-on sensor for Cu2+ and its application in live cell imaging. J. Lumin. 132 (9), 2456–2461.
Wang, M., Yan, F., Zou, Y., Chen, L., Yang, N., Zhou, X., 2014. Recognition of Cu2+ and Hg2+ in physiological conditions by a new rhodamine based dual channel fluorescent probe. Sensor. Actuator. B Chem. 192, 512–521.
Yang, Z., She, M., Yin, B., Cui, J., Zhang, Y., Sun, W., et al., 2011. Three Rhodamine-based "off–on" Chemosensors with high selectivity and sensitivity for Fe3+ imaging in living cells. J. Org. Chem. 77 (2), 1143–1147.
Yuan, Y., Sun, S., Liu, S., Song, X., Peng, X., 2015. Highly sensitive and selective turn-on fluorescent probes for Cu 2+ based on rhodamine B. J. Mater. Chem. B 3 (26), 5261–5265.
Zhang, X., Zhu, Y.Y., 2014. A new fluorescent chemodosimeter for Hg2+-selective detection in aqueous solution based on Hg2+-promoted hydrolysis of rhodamine-glyoxylic acid conjugate. Sensor. Actuator. B Chem. 202, 609–614.
Zhang, X., Huang, X.J., Zhu, Z.J., 2013. A reversible Hg (II)-selective fluorescent chemosensor based on a thioether linked bis-rhodamine. RSC Adv. 3 (47), 24891–24895.
Zhao, Y., Zheng, B., Du, J., Xiao, D., Yang, L., 2011. A fluorescent "turn-on" probe for the dual-channel detection of Hg (II) and Mg (II) and its application of imaging in living cells. Talanta 85 (4), 2194–2201.
Zhu, M., Yuan, M., Liu, X., Xu, J., Lv, J., Huang, C., et al., 2008. Visible near-infrared chemosensor for mercury ion. Org. Lett. 10 (7), 1481–1484.
Zhu, W., Chai, X., Wang, B., Zou, Y., Wang, T., Meng, Q., Wu, Q., 2015. Spiroboronate Si-rhodamine as a near-infrared probe for imaging lysosomes based on the reversible ring-opening process. Chem. Commun. 51 (47), 9608–9611.